

RXJ 215319-1514: Contours from 1992 X-ray data

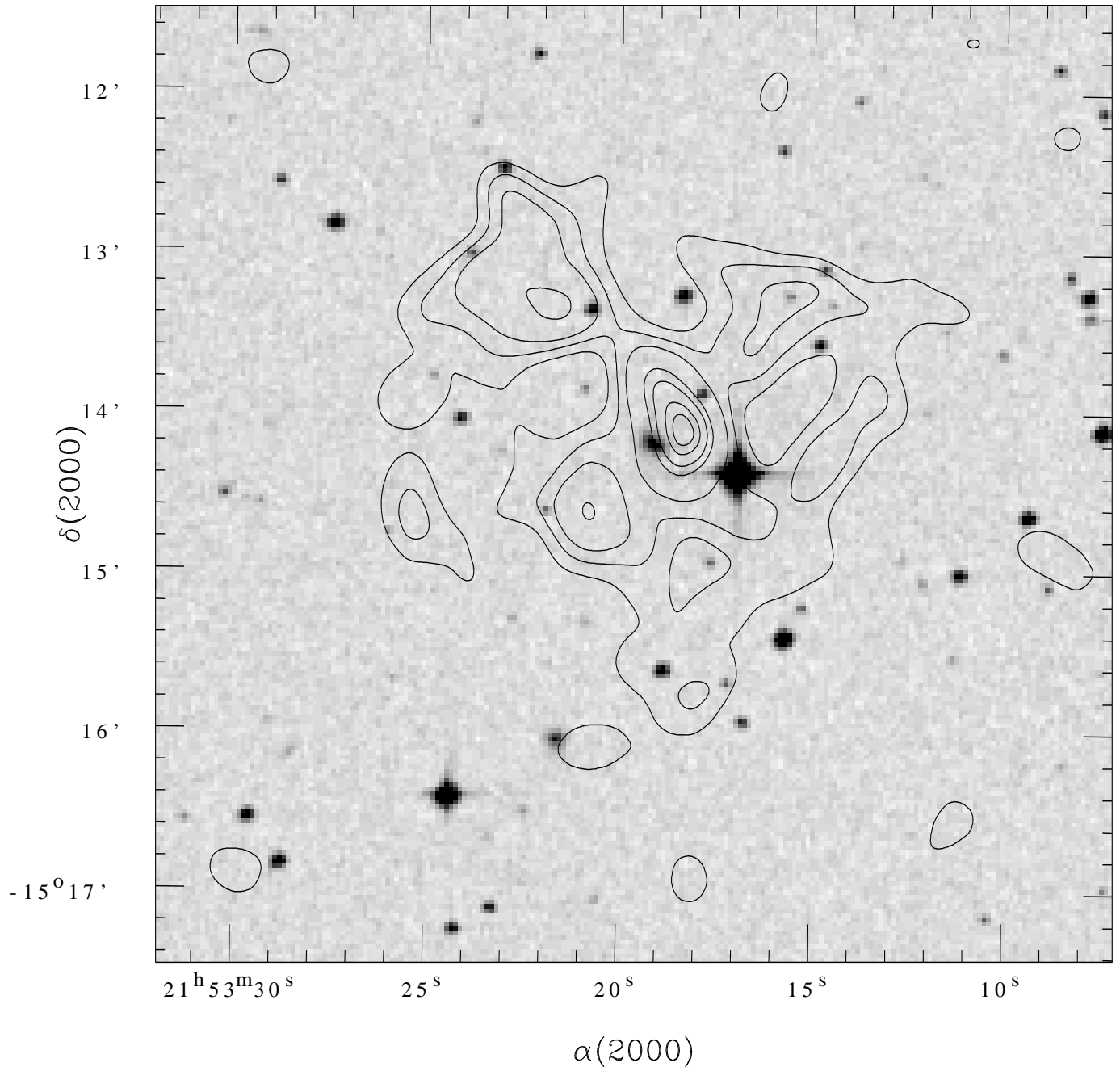
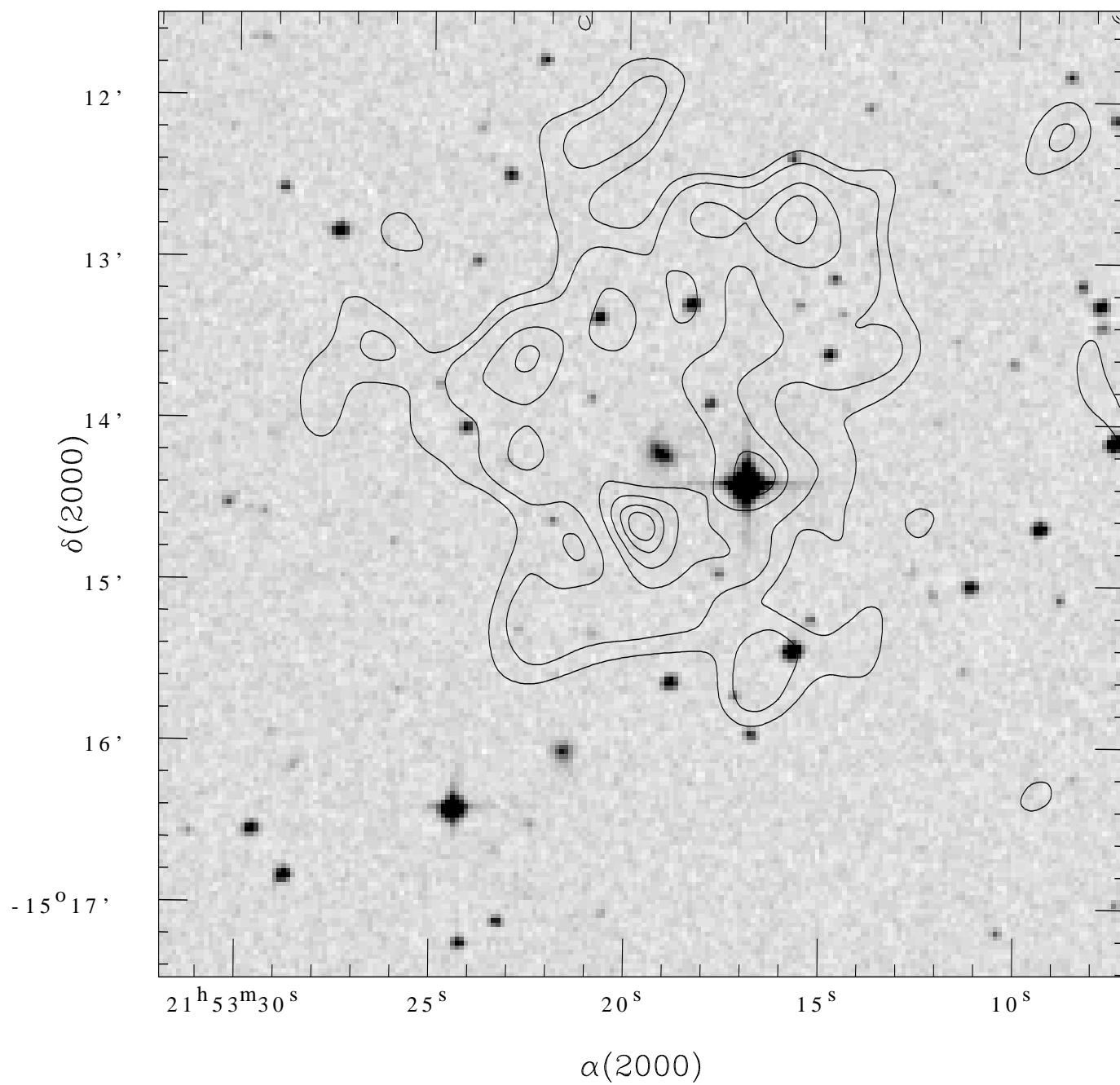


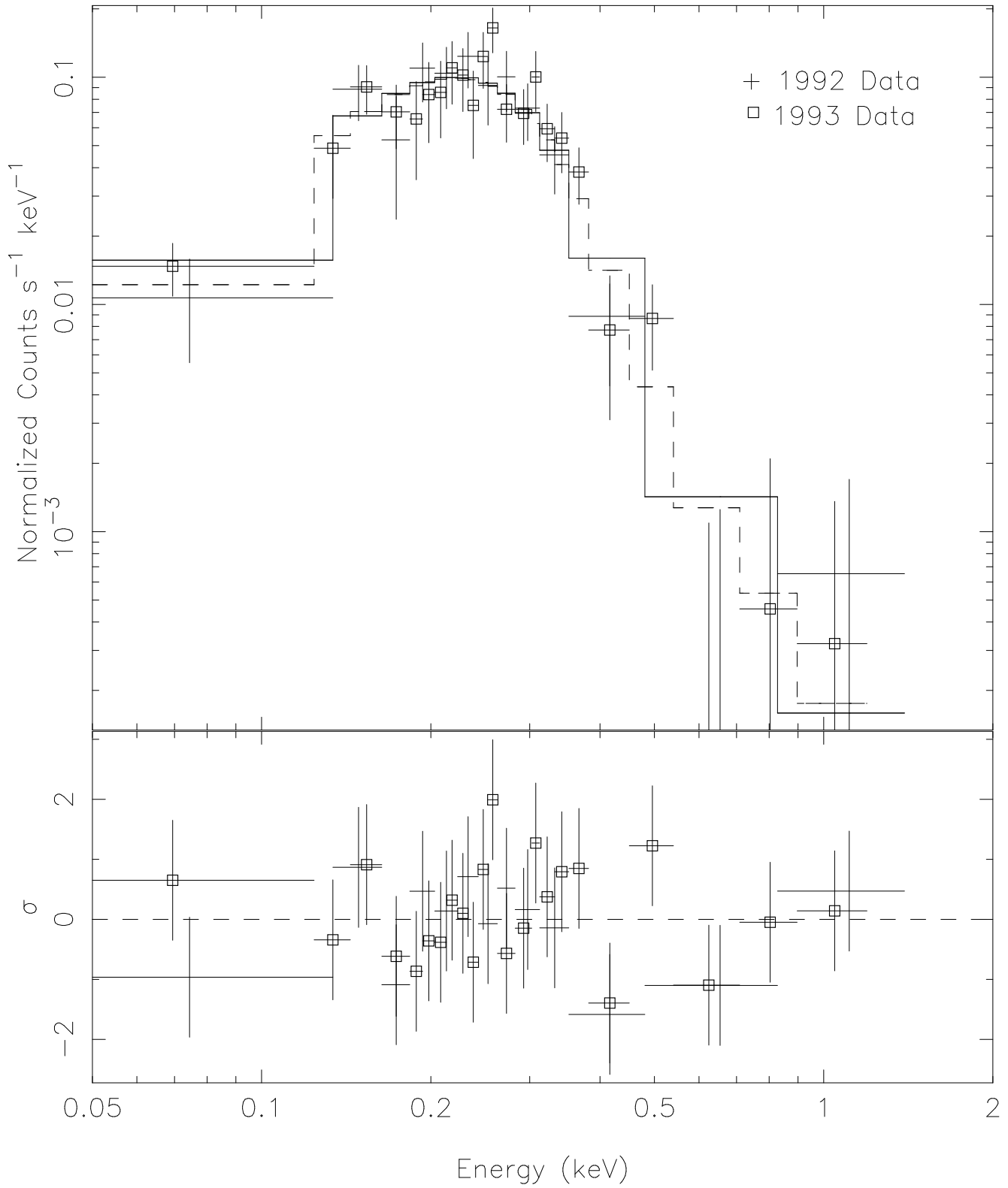
TABLE 1
OPTICAL EMISSION LINE PARAMETERS OF THE NARROW-LINE SY1 GALAXY

Line	Equivalent Width (\AA)	Measured FWHM (\AA)	Intrinsic FWHM (km s^{-1})
NII 6549	1.0 ± 0.3	1.1 ± 0.5	-
H α	40.8 ± 1.0	22.3 ± 1.2	880 ± 50
NII 6583	9.8 ± 0.6	7.8 ± 0.6	180 ± 25

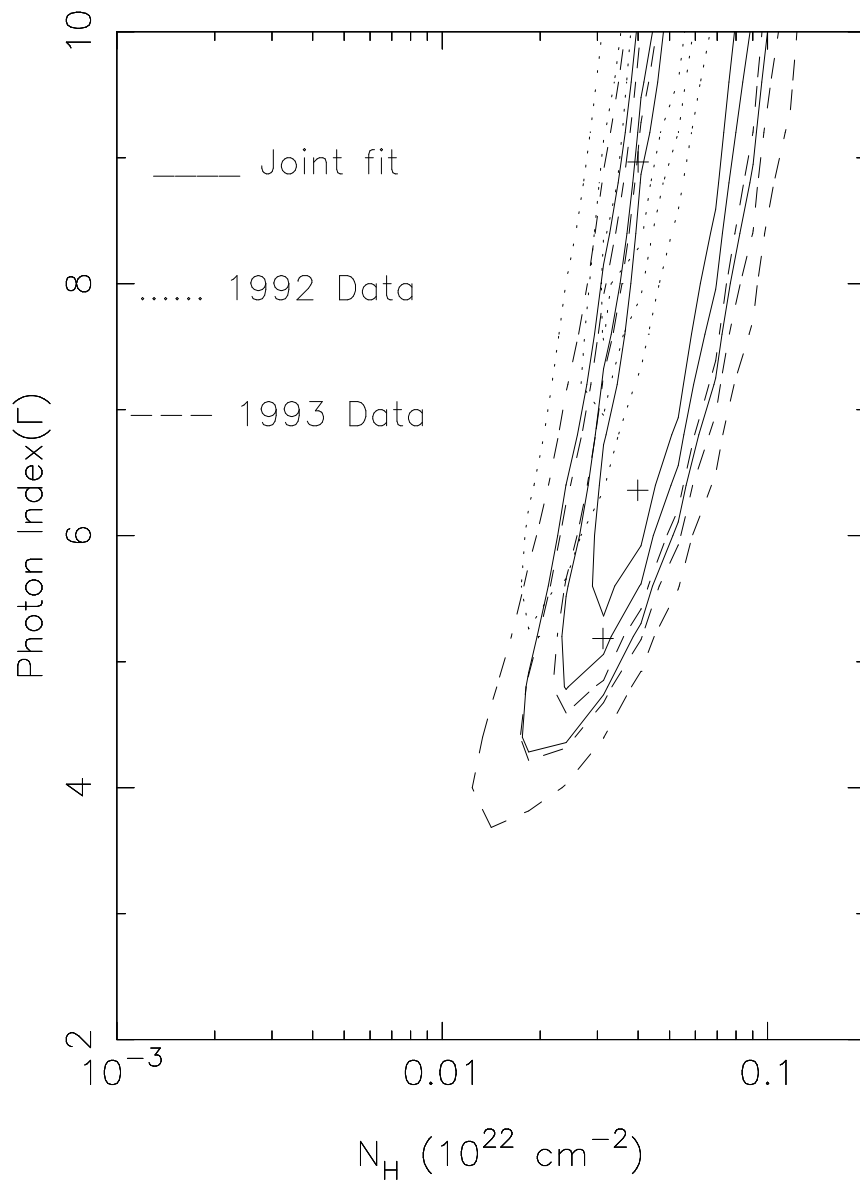
RXJ 215319-1514: Contours from 1993 X-ray data



ROSAT PSPC Data and folded model (RX J2153.3-1514)



Confidence Contours



AN ULTRA-SOFT X-RAY SOURCE (RX 215319-1514) AND DISCOVERY OF A NARROW LINE SEYFERT 1 GALAXY

Kulinder Pal Singh ^{1,3} & Laurence R. Jones ^{2,4}

Received _____; accepted _____

Version Date: September 20, 1999

arXiv:astro-ph/9910486v1 27 Oct 1999

¹Department of Astronomy & Astrophysics, Tata Institute of Fundamental Research,
Mumbai 400005, India

²Department of Physics & Astronomy, University of Birmingham, Birmingham B15 2TT,
U.K.

³singh@tifr.res.in

⁴lrj@star.sr.bham.ac.uk

ABSTRACT

We present results on the identification of the optical counterpart of an ultra-soft X-ray source discovered with *ROSAT*. Two optical candidates – a galaxy and a star, are found within the error circle of the X-ray source position. Optical spectroscopy of the two candidates reveals that a) the galaxy is a narrow-line Seyfert type 1 galaxy, and b) the star is a late A-type or an early F-type. The F_x/F_{opt} ratio is too high for the star to be the counterpart of the X-ray source, but consistent with that for an active galaxy. Although higher resolution X-ray imaging of the region is needed to definitely settle the question of the counterpart of the X-ray source, the narrow-line Seyfert 1 galaxy is the best candidate. The spectral properties of the newly discovered narrow-line Seyfert 1 galaxy are also presented, including its extreme X-ray power law spectral index of $\Gamma \geq 4$.

Subject headings: galaxies:active – galaxies:nuclei – Seyferts individual
(RXJ 2153.3-1514) – X-rays: galaxies

1. INTRODUCTION

The catalogue of ultra-soft X-ray sources of Singh et al. (1995) based on WGACAT (White, Giommi, & Angelini 1994), consists mostly of white dwarfs, cataclysmic variables and some stars. A few extragalactic sources (galaxies and QSOs) which have very steep X-ray spectra and lie in the direction of low interstellar hydrogen column density are also included. These few sources are quite unusual since the ratio of soft (0.1–0.4 keV) and medium energy (0.4–0.9 keV) fluxes is many times larger than for a typical active galaxy or an AGN that they resemble. Although the soft excesses over and above the canonical power-law in Seyferts can cause these galaxies to appear very soft, recent observations with *ROSAT* have shown the existence of intrinsically steep spectrum Seyferts (Brandt, Pounds, & Fink 1995; Boller, Brandt, & Fink 1996; Laor et al. 1997) which have very narrow emission lines and are, therefore, classified as narrow-line Seyfert 1 galaxies. As part of our programme to optically identify the counterparts of ultra-soft sources in the catalogue of Singh et al. (1995), we have discovered a narrow-line Seyfert 1 galaxy which is a strong candidate for being a counterpart of an ultra-soft X-ray source viz., WGA J2153.3-1514 (RXJ 2153.3-1514).

In this paper, we present our analysis of the archival X-ray data on the ultra-soft X-ray source and optical spectroscopic observations of two bright objects within the error circle of the ultra-soft X-ray source. One of these objects is found to be a bright narrow-line Seyfert 1 galaxy at a redshift of 0.0778, and the other is a star.

2. X-RAY DATA AND ANALYSIS

The region of the sky containing this source was observed with the *ROSAT* (Truemper et al. 1983) PSPC detector twice, once from 1992 November 19 to 29 and then from 1993

May 6 to 11. ROSAT X-ray data corresponding to these observations were obtained from the public archives maintained at the High Energy Astrophysics Science Archive Research Center (HEASARC) in USA, and analysed by us. The data are referred by the sequence numbers rp800227n00 and rp800227a01 (rp800227p and rp800227p-1 in the public archives in Germany) for the 1992 and 1993 observations respectively. The effective exposure times were 9040 s and 17436 s in the first and second observation respectively. Abell 2382 was the target source in both the observations. An unidentified ultra-soft X-ray source was detected $\sim 41'$ from the centre of the field in the two sets of observations. The source was not obstructed by the PSPC window support structure. The source is, however, rather weak with a total of 203 ± 22 counts in the first observation, and 375 ± 31 counts in the second observation in the *ROSAT* energy band of 0.1 - 2.4 keV. The source counts were obtained from a circle of radius $2.7'$ centered on the peak position, and after subtracting the background estimated from an annular region with the same center and with inner and outer radii of $4.2'$ and $8.4'$ respectively. This was done using the *imcnts* program in the PROS software package. The large radius for source extraction was necessitated due to the broadening of the point spread function (psf) at large off-axis angle from the centre of the field of view of the telescope. The optimal extraction radius was selected by changing the radius and finding the maximum in the total source counts. The background estimate was checked by increasing the inner and outer radii by a few arcmins and no significant change was found. The X-ray intensity in the two observations is, thus, almost unchanged.

We have extracted data from identical sections of the X-ray image around the ultra-soft source in the two observations. Due to the large off-axis angle of the X-ray source, the psf of the telescope is as large as $1.7'$ (half energy radius) leading to a considerable uncertainty in the position of the source in both the observations. In addition, the weakness of the source does not allow us to correct for any residual pointing errors in the two observations, smaller than the psf. X-ray contour maps made from the individual observations of the

source are shown in Figures 1 and 2 after overlaying on an optical image of the source that was extracted from the Digital Sky Survey (DSS). The raw image was smoothed with a Gaussian ($\sigma = 20$ pixels = $10''$) before plotting in both the cases. The structure seen in the contour maps is unlikely to be real as these can arise due to the large off-axis angle of the source (see Hasinger et al. 1993). A galaxy ($V=14.7$ mag) and a star ($V=11.72$ mag) can both be seen close to the central maximum in the X-ray maps in Figs. 1 and 2. The position of the galaxy, as measured from the DSS, is $RA(2000) = 21^h 53^m 19^s$ and Declination (2000) = $-15^\circ 14' 20''$. The star is identified in the HST Guide Star Catalog as GSC 0637600659 and its position is given as $RA(2000) = 21^h 53^m 16^s.8$, Declination(2000) = $-15^\circ 14' 22.9''$. The X-ray maxima in the two images do not coincide. The separation between the two maxima is, however, only $0.6'$. It is quite clear from Fig. 1 that the galaxy is an X-ray source. X-ray emission from the star, although somewhat unlikely (see §4 below), cannot be ruled out, however. It is very difficult to quantify the contribution of star to the observed X-ray emission, however, using a radial profile of the source we estimate that $\leq 40\%$ of the flux may come from the star if it is indeed an X-ray emitter. No radio source has been reported within $5'$ radius from the X-ray source.

A photon energy spectrum was accumulated from the on-source counts obtained from a circular region on the sky, having a radius of $2.7'$, to account for the large point spread function. The corresponding background spectrum was accumulated from several neighbouring regions at nearly the same off-axis angle as the source. This procedure was applied to the data from both the observations separately. The X-ray spectra from the two observations are nearly identical and are shown together in the upper panel of Figure 3, after regrouping of channels to improve the statistics. Almost all the counts in the spectrum are below 0.5 keV.

We used the XSPEC (Version 10.0) spectral analysis package to fit the data with

spectral models. This requires a knowledge of the response of the telescope and the detector. Using the source spectral files and information about the source off-axis angle contained within them, we generated an auxiliary response file of the effective area of the telescope, by using the program *pcarf* in the FTOOLS (version 4.0) software package. This program uses the available off-axis calibration of the telescope, and the amount of scattering of X-ray photons and their dependence on energy are taken into account. The response matrix *pspcb – gain2 – 256.rm.f*, as provided by the ROSAT GOF at HEASARC, was used to define the energy response of the PSPC. The *ROSAT* PSPC pulse height data were re-grouped to have a minimum of 25 counts per grouped channel and then used for fitting spectral models so that the χ^2 test for finding best fit models could be applied meaningfully. Channels with no useful data, after background subtraction, were ignored. The spectra from the two observations were fitted separately as well as jointly. The two spectra were kept separate to avoid the introduction of any systematic errors. The results of a joint analysis are as follows:

Using a power-law model and absorption due to an intervening medium using absorption cross-sections as given by Morrison & McCammon (1983), we obtain a best fit ($\chi^2_{min} = 24.05$ for 33 degrees of freedom) for a photon index (Γ) of $6.4^{+5}_{-1.5}$ and $N_H = 4^{+3.9}_{-1.4} \times 10^{20} \text{ cm}^{-2}$. The errors quoted, here and below, are with 90% confidence based on $\chi^2_{min} + 2.71$. The best-fit value for N_H is about the same as the 21-cm value ($N_H = 4 \times 10^{20} \text{ cm}^{-2}$) from radio observations in this direction, indicating that all the X-ray absorption is due to matter in our own Galaxy. Based on the best fit model parameters, the total X-ray flux from the source is estimated to be $9.5 \times 10^{-14} \text{ ergs cm}^{-2} \text{ s}^{-1}$ with interstellar absorption, and $1.0 \times 10^{-11} \text{ ergs cm}^{-2} \text{ s}^{-1}$ without intervening absorption in the 0.1–2.0 keV energy band. The large difference between the absorbed and unabsorbed fluxes is due to the very steep spectral index. The best fit power-law model is shown as a histogram in Fig. 3. We have derived the 68%, 90%, and 99% confidence regions for Γ and N_H , based on the joint

analysis of the two spectra, as well as from the analysis of individual spectra, and these confidence regions are shown as contour diagrams in Figure 4. This Figure shows that the results from these analyses are consistent with each other.

Using black-body or thermal plasma emission models gives equally good fits to the spectra. It is, however, difficult to constrain both the temperature and N_{H} independently. Keeping N_{H} fixed at the 21-cm value, we get the best fit ($\chi_{\text{min}}^2 = 22.7$ for 34 degrees of freedom) value of $kT = 30_{-9}^{+9}$ eV, and 0.1–2.0 keV X-ray flux of 7.5×10^{-14} ergs cm^{-2} s^{-1} (with absorption) and 2.7×10^{-12} ergs cm^{-2} s^{-1} (without absorption).

Using a “mekal” optically thin thermal plasma model (Kaastra 1992) with solar abundance also gives an equally good fit to the data with $\chi_{\text{min}}^2 = 24.6$ for 34 degrees of freedom. The best fit $kT = 54_{-12}^{+11}$ eV for fixed $N_{\text{H}} = 4 \times 10^{20}$ cm^{-2} . The 0.1–2.0 keV X-ray flux for these parameters is 1.4×10^{-13} ergs cm^{-2} s^{-1} (with absorption) and 5.3×10^{-12} ergs cm^{-2} s^{-1} (without absorption). As can be seen from the above analyses the flux values are very sensitive to the assumed value of N_{H} and the shape of the spectrum.

3. OPTICAL OBSERVATIONS AND ANALYSIS

Low resolution optical spectra of candidate counterparts were obtained at the Lick 3m telescope on 1995 August 2. A long slit was positioned across the 11th mag star and the nucleus of the 14th mag galaxy, near the peak of the X-ray emission in Fig 1. The slit position angle was 71.1 degrees. The Kast spectrograph was used with a dichroic beam splitter which operated at 5500 Å, sending the blue and red light to blue and red spectrograph arms, each with Reticon CCD detectors. A slit width of 2.5 arcsec and a grism (blue) and a grating (red) both of 600 lines/mm gave a resolution of 6.5 Å (FWHM). The exposure time was 400 sec and the airmass was 2.7.

Flat-fielding and wavelength calibration were performed using appropriate quartz lamp and arc lamp exposures, which were taken frequently through the night. The quartz lamp exposures were scaled and combined to reject cosmic rays and to improve the signal-to-noise ratio. The wavelength calibration was accurate to $\sim 2\text{\AA}$, as measured from night sky lines. Approximate flux calibration was performed using standard *IRAF* procedures via observations of two Kitt Peak spectrophotometric standard stars. We were not able to correct for the loss of blue light due to atmospheric refraction, so the flux calibration is very approximate. Some residual continuum fluctuations are visible at $\lambda > 5500\text{\AA}$ in the spectrum of the star. Atmospheric absorption bands at $\lambda > 6800\text{\AA}$ were removed in the galaxy spectrum using high signal-to-noise observations of bright stars observed at a similar airmass as the target galaxy.

The spectrum of the galaxy is shown in Figure 5. The gap at 5500\AA is due to the effect of the dichroic. Although the spectrum is noisy, [O III] (5007\AA), $H\alpha$ and [N II] emission lines are visible. The redshift derived from Gaussian fits to these three lines is 0.0778 ± 0.0002 . The $H\alpha + [\text{N II}]$ region was fit with three emission lines with fixed centres but variable widths and intensities. The resulting line parameters are given in Table 1. Errors on the line widths were determined from 100 Monte-Carlo simulations of the region.

The parameters of the [N II] 6549 line (and the [O III] line) are not well constrained (the [N II] 6549 FWHM is smaller than the instrumental resolution). The $H\alpha$ line, however, is clearly resolved. After correcting for the instrumental resolution, the intrinsic FWHM is $880 \pm 50\text{ km s}^{-1}$. This value, together with the very soft X-ray spectrum, is indicative of a narrow-line Seyfert 1 galaxy (Boller, Brandt & Fink 1996). We note that although $H\beta$, rather than $H\alpha$, line widths are usually quoted for NLS1s (because $H\beta$ remains unblended at lower resolution), Osterbrock & Pogge (1985) found that the $H\alpha$ and $H\beta$ NLS1 line widths were very similar.

In order to confirm the NLS1 classification, the spectrum was smoothed with a wide boxcar function of width 50\AA to increase the signal-to-noise in broad spectral features, such as the blends of FeII emission lines which form part of the NLS1 definition of e.g., Goodrich (1989). The resulting spectrum is shown in Figure 6. Redshifted FeII 4570\AA , with the expected width of $\approx 200\text{\AA}$, is clearly visible, along with H β , [O III] and a marginal detection of the FeII $5190\text{--}5300\text{\AA}$ blend. The presence of the FeII features confirm the classification as a NLS1 galaxy. The continuum is, however, too poorly defined to reliably measure the emission line parameters at the blue end of the spectrum. A higher signal-to-noise spectrum is clearly needed to investigate the line parameters in more detail.

The star near the X-ray source position, known as GSC 0637600659, has optical magnitudes given as $Q_V=11.72$ and $Q_B=11.82$, in the HST GSC catalog. The spectrum of the star is shown in Figure 7. No emission lines characteristic of an accreting cataclysmic variable are seen in the spectrum. There is also no evidence for chromospheric activity. Based on the spectral characteristics the star is most probably of late-A to early-F spectral type.

4. DISCUSSION

The position of the ultra-soft X-ray source is not well determined in the present observations making the task of optical identification difficult, although two bright optical objects are seen near the X-ray peak position. Multiple sources being responsible for the X-ray emission are, however, unlikely since the $\log N - \log S$ relation (Hasinger, Schmidt, & Truemper 1991) predicts only 10^{-1} sources per square degree with flux (S) $\geq 3 \times 10^{-13}$ ergs $\text{cm}^{-2} \text{ s}^{-1}$ (mean separation $\approx 3^\circ$), and 10^{-3} sources per square degree with flux $\geq 3 \times 10^{-12}$ ergs $\text{cm}^{-2} \text{ s}^{-1}$ (mean separation $\approx 30^\circ$). The probability of two X-ray sources, each with a flux similar to the observed flux, having a separation of $5' - 10'$ is, therefore, quite low.

The ratio of X-ray flux (F_x) to optical flux (F_v) is a very useful tool in the process of optical identification of X-ray sources (see Maccacaro et al. 1988). Using the energy range of 0.3–3.5 keV to calculate the X-ray flux, Maccacaro et al. give the following relationship to estimate the ratio $\log(F_x/F_v)$:

$$\log(F_x/F_v) = \log F_x + m_v/2.5 + 5.37$$

Based on allowed spectral models fitted to the X-ray spectrum, the $\log F_x$ in the 0.3–3.5 keV energy range is estimated to be -13.32 (blackbody spectrum), -13.07 (power-law), and -12.82 (thermal plasma). (The 0.1–2.0 keV fluxes quoted earlier are higher because of the steepness of the spectrum and sensitivity to N_H). Thus, we find that if the X-ray emission is attributed to the star then the flux ratio, $\log(F_x/F_v)$, is in the range -3.26 to -2.76.

Comparing these values with the nomograph given in Figure 1 of Maccacaro et al. (1988), we can see that the flux values and the ratios indicate the star should be of G, K or M-type. Other possibilities are active stars in RSCVn-type binaries (late G to K subgiants or giants) or among rapid rotators (usually dwarf K or dwarf M-types). The optical spectrum (Fig. 7) taken by us, however, clearly shows the star to be a normal A-F type. Besides, active stars do not usually have such a soft X-ray spectrum (Singh et al. 1999). Even solar-types have $kT=0.3$ keV and L_x/L_v of $\sim 10^{-7}$ – 10^{-6} (Mewe et al. 1998). For the star to be as soft as it is in X-rays it must harbor either a white dwarf or be a cataclysmic variable of some kind, but the optical spectrum shows only the signature of a normal star.

The narrow-line Seyfert 1 (NLS1) galaxy has $V \simeq 14.7$ and if it is the source of X-rays then $\log(F_x/F_v)$ is in the range -2.07 to -1.57, if the total flux can be attributed to it. This ratio is well in the range observed for galaxies and low luminosity AGN (even if only 60% of the total flux is from the galaxy). The optical spectrum of the galaxy shows an $H\alpha$ emission line with a width intermediate between those of Sy1 and Sy2 galaxies, typical of NLS1s. Such galaxies are known to have steep soft X-ray spectra. For the observed redshift and

assuming $H_0=75 \text{ km s}^{-1} \text{ Mpc}^{-1}$, $q_0=0$ in a Friedmann cosmology, the luminosity distance of the Seyfert galaxy is 323.3 Mpc. The (unabsorbed) X-ray luminosity of the Seyfert galaxy in the 0.1–2.0 keV energy band is $3.4 \times 10^{43} \text{ ergs s}^{-1}$ for a blackbody spectrum, $1.25 \times 10^{44} \text{ ergs s}^{-1}$ for a power-law type spectrum, and $6.6 \times 10^{43} \text{ ergs s}^{-1}$ for a thermal plasma. This X-ray luminosity is quite typical of Seyfert galaxies. The observed X-ray source is, therefore, very likely to be associated with this narrow emission line galaxy at a redshift of 0.0778.

The value of the X-ray spectral index, $\Gamma \geq 4$ (99% confidence), is extreme even for the NLS1 class of AGN, being steeper than any of the galaxies in the compilation of Boller et al. (1996). The position on the Γ - $H\beta$ line width plane (Fig. 8 of Boller et al) is, however, consistent with an extrapolation based on the other NLS1 galaxies.

5. CONCLUSIONS

A narrow-line Seyfert 1 galaxy has been discovered in the error circle of an ultra-soft X-ray source. Although higher spatial resolution and broad-band X-ray observations are needed to be certain about the association of this galaxy with the ultra-soft X-ray source, based on the spectral characteristics it appears to be the better candidate for being the counterpart of the X-ray source than the bright A–F type star which is also in the error circle. Assuming this association to be true, the 0.1–2.0 keV X-ray luminosity of the NLS1 is in the range of $(3.4\text{--}12.5) \times 10^{43} \text{ ergs s}^{-1}$, and its soft X-ray spectral index is extremely steep ($\Gamma \geq 4$).

This research has made use of the PROS software package provided by the ROSAT Science Data Center at Smithsonian Astrophysical Observatory, and the FTOOLS software package provided by the High Energy Astrophysics Science Archive Research Center (HEASARC) of NASA’s Goddard Space Flight Center.

REFERENCES

- Boller, T., Brandt, W.N., & Fink, H.H., 1996, *A&A*, 305, 53
- Brandt, W.N., Pounds, K.A., & Fink, H.H., 1995, *MNRAS*, 273, L47
- Goodrich, R.W. 1989, *ApJ*, 342, 224
- Hasinger, G., Schmidt, M., & Truemper, J., 1991, *A&A*, 246, L2
- Hasinger, G., Boese, G., Predehl, P., Turner, T.J., Yusaf, R., George, I.M., & Rohrbach, G. 1993, MPE/OGIP Calibration Memo CAL/ROS/93-015 on “The Off-axis point spread function of ROSAT PSPC”.
- Kaastra, J.S. 1992, An X-ray Spectral Code for Optically Thin Plasmas (Ver 2.0; SRON-Leiden Rep.)
- Laor, A., Fiore, F., Elvis, M., Wilkes, B.J. & McDowell, J.C., 1997, *ApJ*, 477, 93
- Maccacaro, T., Gioia, I.M., Wolter, A., Zamorani, G., & Stocke, J.T., 1988, *ApJ*, 326, 680
- Mewe, R., Drake, S.A., Kaastra, J.S., Schrijver, C.J., Drake, J.J., Guedel, M., Schmitt, J.H.M.M., Singh, K.P., & White, N.E., *A&A*, 1998, 339, 545
- Morrison, R. & McCammon, D., 1983, *ApJ*, 270, 119
- Osterbrock, D.E. & Pogge, R.W., 1985, *ApJ* 297, 166.
- Singh, K.P., Barrett, P., White, N.E., Giommi, P., & Angelini, L., 1995, *ApJ*, 455, 456
- Singh, K.P., Drake, S.A., Gotthelf, E.V., & White, N.E., 1999, *ApJ*, 512, 874.
- Truemper, J., 1983, *Adv. Space Res.*, 2, 241
- White, N.E., Giommi, P., & Angelini, L., 1994, *IAU Circ. No.* 6100

Fig. 1.— X-ray image of RX 215319-1514.6 as observed with the *ROSAT* PSPC in 1992 observations after smoothing with a Gaussian ($\sigma=10''$) and overlaid on the optical image (gray) obtained from the Digital Sky Survey. X-ray contours are plotted at 30, 40, 50, 70, 80, 90 and 95% of the peak brightness of 0.0049 counts pixel⁻¹. (1 pixel =0.5'' \times 0.5'')

Fig. 2.— X-ray image of RX 215319-1514.6 as observed with the *ROSAT* PSPC in 1993 observations after smoothing with a Gaussian ($\sigma=10''$) and overlaid on the optical image (gray) obtained from the Digital Sky Survey. X-ray contours are plotted at 40, 50, 70, 80, 90 and 95% of the peak brightness of 0.0066 counts pixel⁻¹. (1 pixel =0.5'' \times 0.5'')

Fig. 3.— *ROSAT* PSPC X-ray spectra of the ultra-soft X-ray source obtained from two observations and fitted jointly with a power-law model are shown in the upper panel. The best fit power-law model from a joint fit is shown as histograms. The significance of the residuals between the observed data points and the model are shown in the lower panel.

Fig. 4.— Allowed ranges of the power-law photon index Γ and N_H for 68%, 90%, and 99% confidence based on counting statistics. The '+' marks the best fit value.

Fig. 5.— Optical spectrum of the active galaxy. Prominent emission lines are labelled. The gap at 5500Å is instrumental. The spectrum has been smoothed with a box of size 3 pixels (6.9Å) corresponding to the instrumental resolution.

Fig. 6.— Same as in Fig.5 but smoothed with a box of size 50Å.

Fig. 7.— Optical spectrum of the star, GSC 0637600659.

